JOURNAL OF CATALYSIS **141**, 102–113 (1993)

The Active Surface Species in Alkali-Catalyzed Carbon Gasification: Phenolate (C–O–M) Groups vs Clusters (Particles)

S. G. CHEN AND R. T. YANG[1]

Department of Chemical Engineering, State University of New York at Buffalo, Buffalo, New York 14260

Received August 20, 1992

The activities and catalytic roles of different species of potassium in the gasification reactions of graphite by H_2O and CO_2 are investigated. TEM techniques are used to measure the rates of monolayer edge recession (uncatalyzed and C–O–K catalyzed) and rates of monolayer channeling (catalyzed by particles) on the basal plane of graphite reacting with 21 Torr H_2O at 700°C. The turnover frequencies for carbon gasification are: 0.08 s^{-1} (uncatalyzed), 0.15 s^{-1} (catalyzed by C–O–K groups), and 7.8 s^{-1} (catalyzed by particles). Thus the particles have a high activity, whereas the C–O–K groups have only a small activity. TGA and literature results using mixtures of carbon and alkali salts show a sigmoidal dependence of gasification rates on catalyst loading. This is the result of catalyst dispersion and competition between the C–O–K groups and alkali particles. A CNDO semi-empirical molecular orbital calculation is performed on model graphite substrates with -O and -O-K groups bonded to the $\{10\bar{1}l\}$ zigzag face and $\{11\bar{2}l\}$ armchair face. On the zigzag face, the carbon atom bridging two C–O–K groups gains a large negative charge (-0.486) and hence is a favorable site for binding an O atom. The surface C–C bonds in this structure are substantially weakened by adding O atoms on the bridging C atoms, leading to CO release. The O atoms are supplied by the dissociation of H_2O and CO_2. The possible reason for the alkali particles being more active than the C–O–M (where M = alkali) groups is that the particles can dissociate H_2O and CO_2 at higher rates, by providing either more active sites or higher activities. The CNDO results also predict that the C–O–K groups have an inhibiting effect on the armchair face; an inhibiting effect has indeed been observed earlier in our laboratory.

INTRODUCTION

Alkali and alkaline earth are the best catalysts for the gasification reactions of carbon by CO_2 (to form CO) and H_2O (to form H_2 and CO), which are the bases of coal gasification processes. Because of its importance, a voluminous literature has been devoted to this area and much progress has been made during the past 2 decades toward the understanding of the mechanisms of these catalyzed reactions, possible active intermediates, and phenomena involved in catalyst behaviors.

Many kinds of intermediates and mechanisms have been proposed for different catalysts and reviews on the subject can be found in the literature (*1–7*). Among all the alkali and alkaline earth salts, potassium is the most extensively studied (due to its practical importance). The proposed intermediates for potassium catalysts include metallic K (*8*), K_2O (*8–10*) K_2O_2 (*11*), K_2CO_3 (*8, 9*), K–O–C (*12–19*), and clusters (*16, 20, 21*). Of these active intermediates, the C–O–K type groups have received wide attention.

Many researchers (*12–19*) have suggested and some (*12–17*) have shown evidence for the existence of the C–O–M phenolate groups (here M stands for the alkali or alkaline earth metal atom) on the catalyst surface under gasification conditions. Mims and Pabst (*13, 15, 16*) were the first to suggest and investigate this type of intermediate. Using a combination of surface derivatization (methylation) and solid-state ^{13}C

---

[1] To whom correspondence should be addressed.

0021-9517/93 $5.00

NMR, they demonstrated that under carbon gasification conditions (770–1000 K), a significant fraction (approximately one-quarter) of the potassium in the K_2CO_3 catalyst was bonded to the carbon surface in the form of surface salt complexes which were characterized as C–O–K groups (phenolates). They further studied (*16*) the catalytic role of this type of surface species and showed that these groups were stable at up to 1000 K but at higher temperatures significant amounts of the potassium would slowly vaporize. Using FTIR, both Freriks *et al.* (*14*) and Yuh and Wolf (*17*) observed the possible phenolate intermediates on surfaces of different coal chars and carbons. The infrared spectra of carbon samples prepared under gasification conditions (500 and 750°C) also showed evidence for the existence of C–O–K groups.

The recent study of Meijer *et al.* (*19*) suggested that the active intermediate was in the form of clusters with varying sizes (depending on the K/C atomic ratio) and that the clusters were anchored by phenolate groups to the carbon surface.

From the above discussion, it becomes evident that the phenolate (C–O–M) groups do exist and are likely active. It is also evident that the catalyst behavior, or the forms of intermediate, depends largely on the *dispersion* of the catalyst. The phenolate groups comprise only a fraction of the catalyst; the remainder is in the form of clusters or particles. The sizes of the clusters or particles range from tens of angstroms to micrometers. The clusters or particles possess immense catalytic activities, and their behaviors and the catalytic mechanisms have been studied extensively by using microscopies.

A unique and most intriguing phenomenon associated with the catalyzed gas–carbon reactions is the motion of the catalyst particles which results in the catalytic activity. Using graphite as the carbon, three major catalyst actions have been observed, which are described as follows. (1) Deep channeling: Catalyst particles carve deep, multi-graphite-layer channels on the basal plane of graphite to gasify carbon (*7, 22–25*). (The extensive work by Baker has been reviewed in (*7*).) (2) Monolayer channeling: Catalyst particles carve mono-graphite-layer channels to gasify carbon (*26–32*). These channels are abundant, and propagate at high speeds, contributing significantly to the overall gasification rates. Direct observation of the monolayer channeling has been made with STM recently (*33*). (3) Pitting and edge recession: Catalysts form deep pits on both basal plane and edge planes (*1, 7*). Edge recession is an action similar to channeling; it can involve both multilayer edge (*7*) and monolayer edge (*30*).

The important question that remains to be answered is the relative activities of particles (clusters) as compared to the phenolate groups. This study was designed to provide a direct, quantitative comparison between the activities of these two catalyst species. Moreover, a fundamental understanding of the catalytic activity is also given by a CNDO molecular orbital study.

EXPERIMENTAL

When the basal plane of graphite is exposed to a reactant gas atmosphere, vacancies on the basal plane are expanded (or etched) into pits because the edge carbon atoms have a free sp^2 electron and are the active sites for gasification. The edge sites can be decorated with gold nuclei which are visible in the TEM (*5, 22*). This experimental technique was adopted to study the catalyzed gas–carbon reactions, more specifically, the monolayer channeling action by catalyst particles (*26–32*). Since the active carbon sites are well defined, in both cases, the turnover rates can be measured (*5, 26–32*). These techniques were employed in this study.

The experimental strategy for directly comparing the turnover frequencies catalyzed by C–O–K groups and by particles is as follows. Uncatalyzed etch pits are first formed. Potassium catalyst was introduced under conditions most favorable for the formation of the C–O–K groups. Further reaction will show accelerated etch pit expansion (due to the C–O–K groups on the edges) as well as monolayer channels (by particles which initiate channels from the pit edges). The results of this experiment will yield turnover frequencies for the uncatalyzed reaction, reaction catalyzed by C–O–K, and reaction catalyzed by particles.

A natural single-crystal graphite from Ticonderoga, New York, was used for the TEM study. The reason for choosing this graphite and a detailed explanation of the techniques used for preparing the crystals for reactions, catalyst loading, and subsequent gold decoration have been given elsewhere (*5*, *26–32*). A TGA study was also conducted using a polycrystalline, high-purity graphite. This graphite was nuclear grade (H-451), with less than 100 ppm "ash content" and a surface area of 4.1 m^2/g.

The catalyst precursor was KNO_3, and was puratronic grade supplied by Alfa Products (Danvers, MA) with a purity well above 99.9%. The CO_2 and N_2, used for gasification (the TGA experiment) and as a carrier, respectively, were both of ultrahigh purity grade (99.99% minimum purity for both), and were both subjected to further purification to remove traces of O_2 by passing through a bed of copper turnings at 550°C. For the TEM samples, the catalyst was dispersed on the basal plane of graphite from aqueous solution. The graphite sample was placed on a filter paper on which the solution was dispensed. After air drying, the catalysts were dispersed on the basal plane, as confirmed by optical microscopy.

The graphite samples (with or without catalyst) were placed on a sapphire plate held in an alumina combustion boat. The boat was placed in a quartz tube reactor. Prior to reaction, it was necessary to degas the basal plane of graphite in N_2 at 500°C overnight (*5*). After degassing, the temperature was raised to the reaction temperature and the gas was switched to the reactant (in this experiment, water vapor saturated in N_2 was used) and the samples were reacted for a desired period of time.

In order to obtain graphite samples with edge sites covered by the C–O–K groups, the following experimental procedure was adopted. First, the samples without catalyst were reacted for 2 h at 730°C. Etch pits (with hexagonal shapes, Ref. (*5*)) were created by water vapor. The KNO_3 catalyst was then deposited on some of the samples using the method described above. The remaining samples were without catalyst in order to obtain the uncatalyzed turnover frequency under the same reaction conditions. Dilute KNO_3 solutions were used to avoid congested channels on the basal plane. Both samples (with and without catalyst) were subsequently subjected to reaction (for 3 h).

For the TGA study, the nuclear graphite was first ground to a powder, and impregnated with KNO_3 from a dilute solution. The K/C ratio was controlled by the ratio of the catalyst precursor to graphite. Very dilute solutions were used since low K/C ratios were desired. The mixtures were dried in air at 120°C. In each experiment, 80 mg sample was used.

RESULTS AND DISCUSSION

TEM: Turnover Frequencies of Uncatalyzed, C–O–K Catalyzed, and Particle-Catalyzed Reactions

Figure 1 is a TEM picture of the etch pits formed on the basal plane of graphite. The pits were decorated with gold nuclei, and only the gold nuclei were visible in the TEM (*5*). The pits were formed by reacting with water vapor, at 21 Torr partial pressure and 730°C for 2 h. These pits were monolayer (one graphite layer deep), hexagonal in shape, and were bounded by zigzag edges of graphite (*5*). The turnover frequency calculated from this result was 0.13 C atom/C atom/s (or s^{-1}).

Figure 2 is the TEM picture of the gold-decorated etch pits on graphite which was further reacted with H_2O (21 Torr) at 700°C for 3 h, after first reaction at 730°C for 2 h.

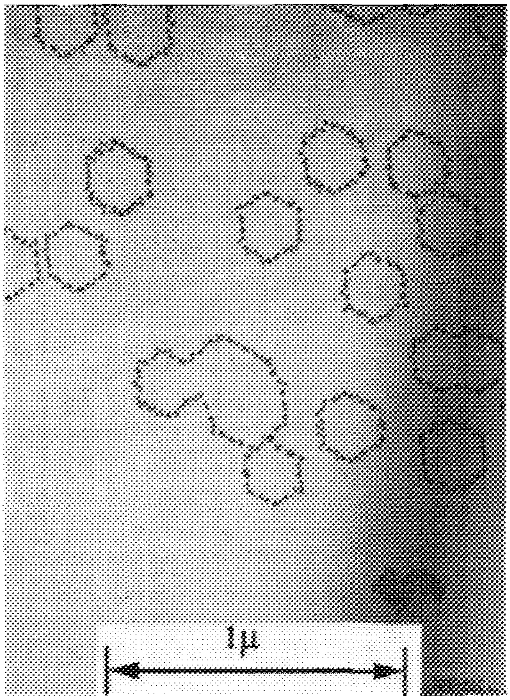

FIG. 1. TEM picture of monolayer etch pits (decorated by gold nuclei) on graphite basal plane after reaction in 21 Torr H_2O at 730°C for 2 h. The pits are bounded by zigzag faces.

From the difference between the sizes in Figs. 1 and 2, the turnover frequency for 700°C (at 21 Torr H_2O) was 0.08 s^{-1}.

The reacted samples shown in Fig. 1 were further dispersed with KNO_3 (which decomposed well below the subsequent 700°C reaction temperature) and subjected to further reaction with H_2O (21 Torr) at 700°C for 2 h. It has been shown that C–O–K groups were formed on the carbon surface under this reaction condition (*12–19*). These reacted samples were decorated with gold nuclei and examined in a TEM. The TEM picture is shown in Fig. 3. The pits in Figs. 2 and 3 could be directly compared, since they were subjected to the same reaction history, with the only difference in the added potassium catalyst. The pits in Fig. 3 were irregular in shape; however, they were larger in all directions as compared to the pits in Fig. 2, the uncatalyzed pits. Figure 3 also shows channels carved by catalyst particles. These were monolayer channels, initiated from the edges of the monolayer etch pits (*32*).

From the results of the catalyzed reaction (Fig. 3), one may obtain information on rates catalyzed by the C–O–K groups as well as that catalyzed by particles. As mentioned, the pits in Fig. 3 were larger, due to catalyzed edge recession. As will become clear later, the C–O–K groups had the lowest catalytic activity; the activity increased as the size of potassium cluster or amount of potassium was increased over the C–O–K groups. Therefore, the turnover frequency for the C–O–K catalyzed reaction could be calculated from the narrowest portions of the etch pits. The value obtained in this manner was 0.15 ± 0.03 s^{-1}. This value was

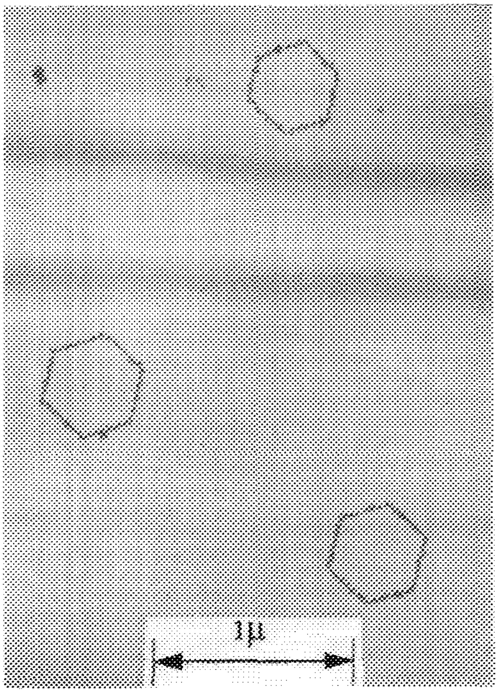

FIG. 2. TEM picture of monolayer etch pits on graphite basal plane. The sample was reacted with 21 Torr H_2O first at 730°C for 2 h followed by 3 h at 700°C, and then gold-decorated.

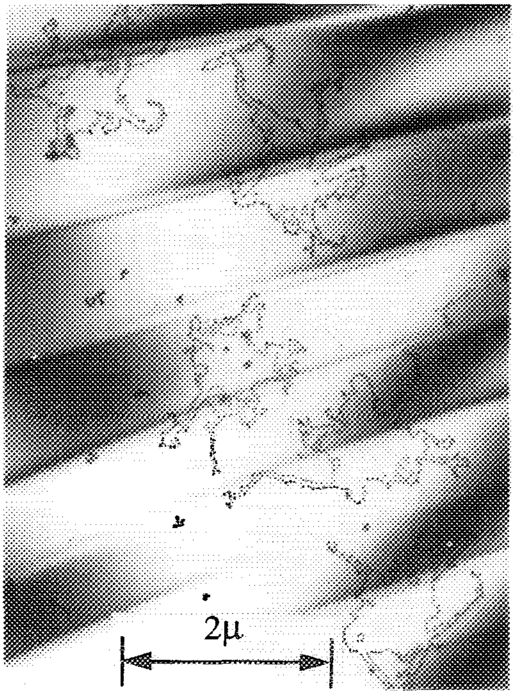

FIG. 3. TEM picture of monolayer etch pits on graphite basal plane. The sample was reacted in 21 Torr H_2O first at 730°C for 2 h followed by KNO_3 deposition and further reaction at 700°C for 3 h before gold decoration for TEM.

nearly twice that of the uncatalyzed reaction, 0.08 s^{-1}.

The turnover frequency for the reaction catalyzed by particles could be calculated from the channel length (*27–32*). Here the longest channel was used because not all channels were initiated from the start of the reaction; e.g., some particles migrated to the edges of the pits where channeling could be initiated. From the longest channels, the turnover frequency was 7.8 ± 0.5 s^{-1}. This value was slightly lower than that measured in a previous study in which 8.5 ± 0.4 s^{-1} was obtained for 690°C (*32*). The difference was likely caused by different loadings and hence different dispersions of the catalyst.

The monolayer (and deep-layer) channels carved by alkali and alkaline earth catalysts were unique in that they had a fluted appearance (Fig. 3 and Ref. (*32*)). Since the two sides of the channel were covered by C–O–M groups, it was possible to estimate the ratio of rates catalyzed by the particle and by C–O–M groups, from the shape of the fluted channel (*32*). For the $C/H_2O/K$ system, the estimated ratio was in the range 30–50 (*32*), which was close to the value of 52 observed in this study.

TGA: Sigmoidal Dependence of Rate on K/C

The dependence of gasification rate on the amount of catalyst loading, expressed in K/C atomic ratio, was measured using thermogravimetric analysis (TGA). The nuclear graphite was used as the carbon sample. Because the rates were too low with 21 Torr H_2O, CO_2 at 1 atm was used as the gaseous reactant. The results are shown in Fig. 4.

The range of K/C was 0–0.005, because the rates leveled off beyond this range. The rates changed significantly at small burnoff and large burnoff levels. For this reason, rates at 10–15% burnoff, where the rates were relatively steady, were taken.

The results shown in Fig. 4 exhibit a sigmoidal behavior. A review of the literature revealed that this behavior was also observed for a number of carbons and for both

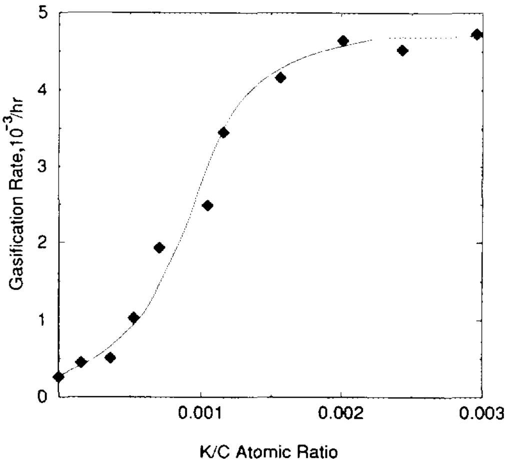

FIG. 4. Gasification rate (in g/g/h) of graphite powder impregnated with KNO_3 (which decomposed upon heating) in 1 atm CO_2 at 700°C.

H_2O and CO_2 reactants, with a variety of alkali salt catalysts (*16, 19, 34, 35*), although this behavior has not been explained. The ratio of K/C at which the gasification rate levels off depends on the gas–carbon system as well as the catalyst and reaction conditions. However, the most important factor appears to be the surface area of the carbon. For example, with an activated carbon (which had a large surface area), the level-off point was 0.05–0.1 K/C ratio (*19*), whereas for nuclear graphite (with a low surface area), Fig. 4 shows a level-off point of approximately 0.002.

The TEM results, discussed above, show that the C–O–K groups have only a small catalytic activity, whereas the particles or clusters have considerably higher activities. This result can be used to interpret the sigmoidal behavior. At very low catalyst loadings, the catalyst is dispersed on the surface carbon atoms to form C–O–K groups. Increasing the catalyst loading will only increase the activity slightly due to the low activity of the C–O–K groups. Further increasing the catalyst loading will result in nucleation and clustering of the catalyst, forming clusters and particles which have high activities. Thus a steep rise in rates with K/C occurs in this range of loading. Upon still further increase in catalyst, the carbon surfaces will be saturated with particles, which will not increase the rates. In fact, this can lead to a further increase in the particle sizes, resulting in a decline in the gasification rates, which has also been observed (*34*). The locations of the turning points in the sigmoidal curve depend on the dispersion of the catalyst and the surface area of the carbon.

This interpretation is in agreement with the methylation results of Mims and Pabst (*16*), which showed that the C–O–K groups increased with K/C ratio most rapidly in the low K/C range, followed by slower increases and an eventual decrease.

According to the above interpretation, one would expect that different heat pretreatments of the catalyst/carbon samples would result in different catalyzed gasification rates due to different dispersions of the catalyst. This was indeed observed by Wigmans *et al.* (*36*) (although they attributed their results to catalyst vaporization and solid-state reaction between carbon and alkali). In their experiment, alkali/carbon samples were heat treated (for 30 min) at 752, 802, and 852°C, before reaction with H_2O at 752°C. The pretreatments at higher temperatures resulted in large decreases in rates. The interpretation based on our results is that pretreatment at a higher temperature leads to better alkali dispersion, hence more C–O–K groups and less clusters and particles are formed on the carbon surfaces.

Origin of Activity of C–O–K Groups

A molecular orbital (MO) calculation was performed in order to provide an understanding of the origin of the catalytic activity of the C–O–K groups for the carbon gasification reactions by H_2O and CO_2. The MO method used here was the semi-empirical CNDO (Complete Neglect Differential Overlap) approximation of Pople and Beveridge (*27*). The CNDO method can give correct geometry and dipole moments (*38*). The computer program used in this work was QCPE No. 584 provided by the Quantum Chemistry Program Exchange Center of Indiana University. In this program, the CNDO parameters of oxygen and carbon were given, but not for potassium. A set of CNDO parameters was available from Hojer and Meza (*39*). Since different CNDO parameters for the same elements were given by different sources, all parameters from Hojer and Meza were used for the ensembles containing potassium, for consistency reason.

The main active sites on graphite are on the two edge planes: $\{10\bar{1}l\}$ or zigzag face and $\{11\bar{2}l)$ or armchair face. Thus, C–O–K groups on these two edge sites were considered, shown in Figs. 5 and 6, respectively. Each figure shows four structures; Structures 1 and 2 were used to compare the local-

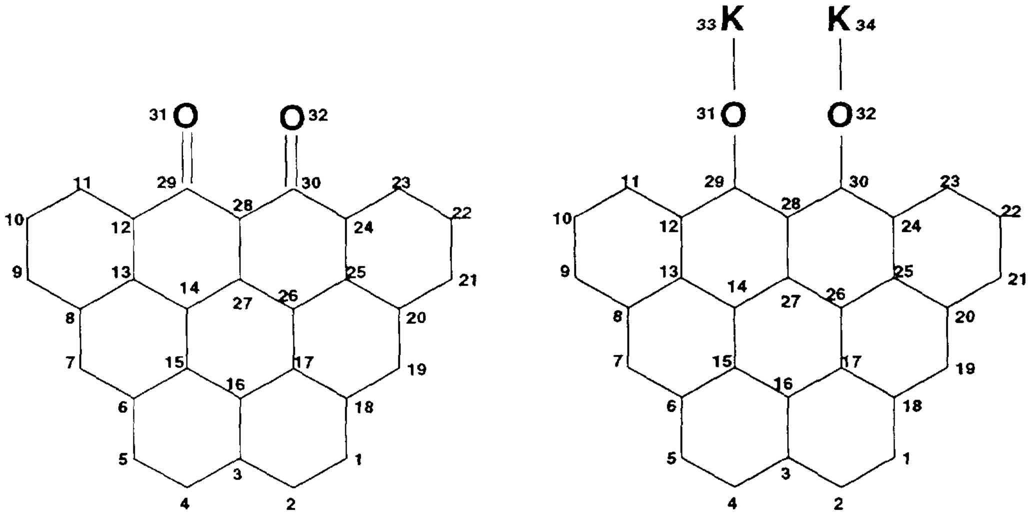

Structure 1

Structure 2

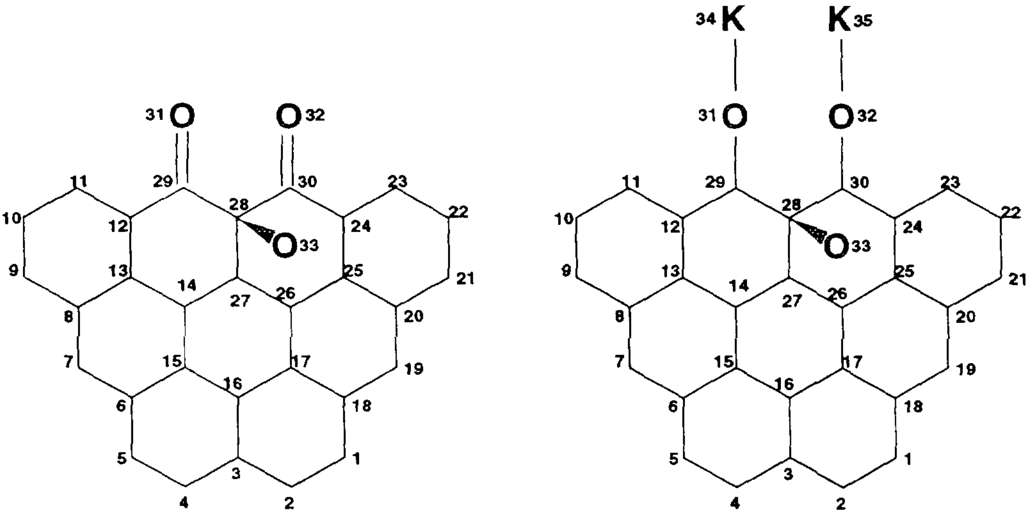

Structure 3

Structure 4

FIG. 5. Model substrates with zigzag face on graphite for CNDO molecular orbital calculation.

ized electron densities, whereas Structures 3 and 4 were used to compare the C–C bond strengths when additional oxygen atoms were attached. The largest sizes of the model substrates shown in Figs. 5 and 6, considering the symmetry, contained nearly 186 atomic orbitals, which was the maximum number allowed by the program. This limited the number of C–O and C–O–K groups on the substrates. Another model substrate with all edge sites saturated by hydrogen atoms, as done by Hayns (*40*),

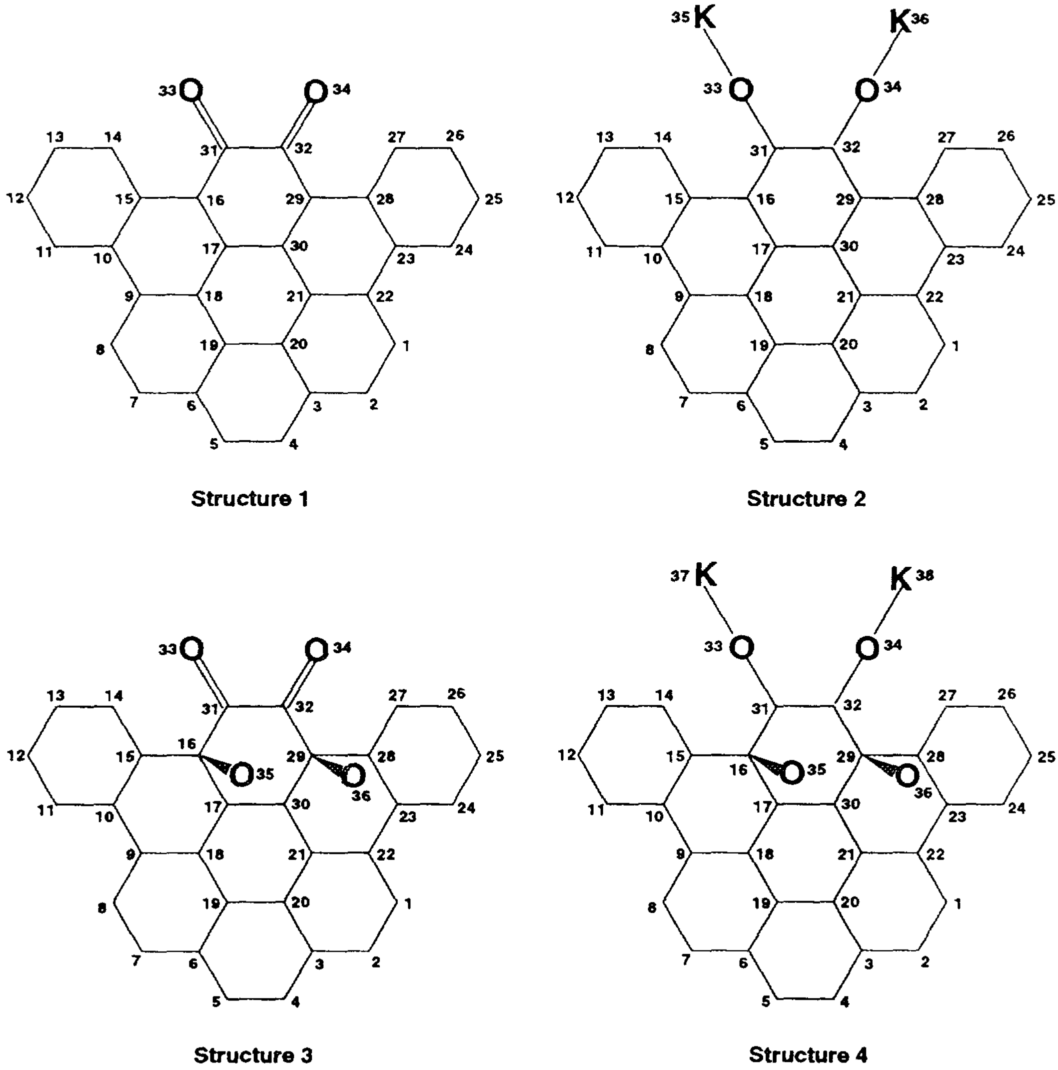

Structure 1

Structure 2

Structure 3

Structure 4

FIG. 6. Model substrates with armchair face on graphite for CNDO molecular orbital calculation.

was also included in calculation. But for the carbon atoms of interest to this work, little differences were found. Experimental values for C–C bond length (1.42 Å) and angle (120°) were used, and these values were fixed. Geometry optimization (for the lowest total energy) was performed to determine the bond lengths for C–O, O–K, and C–C when one of the carbon atoms was also bonded to an O atom. The bond angles were fixed, as shown in Figs. 5 and 6. The O–K bonds might not be in-plane; but the effects caused by the out-of-plane O–K bonds were expected to be negligible or small. The out-of-plane O atoms (O_{33} in Fig. 5 and O_{35} and O_{36} in Fig. 6) formed bonds normal to the graphite basal plane.

The CNDO results will be reported in terms of electron net charge and diatomic energy. The net charge for an atom is defined as:

$N(e)$ = localized electron population
− number of electrons in valence shell;

TABLE 1

Net Charge (Electrons) of Carbon Atoms in Substrates with Zigzag Edge (see Fig. 5)

Number	Structure 1	Structure 2	Number	Structure 1	Structure 2
12	0.1579	−0.1548	25	0.2401	−0.0626
13	0.2401	−0.0626	26	0.1359	−0.1605
14	0.1359	−0.1605	27	0.3211	−0.1867
24	0.1579	−0.1548	28	−0.0128	−0.4863

for carbon atoms,

$$N(\mathrm{e}) = \text{localized electron population } -4.$$

The C–C bond strengths were represented by the diatomic energies. The diatomic energy calculated by CNDO is the contribution to the total energy by any of two atoms in the substrate (*39*). It is not equal to the bond energy, but can be used for direct comparison of bond strengths.

The net charges of different carbon atoms are given in Tables 1 and 2. The results indicated that the chemisorption of O atoms on the edges, for both zigzag and armchair edges, caused positive charges—i.e., deficiency of electrons—on the carbon atoms. However, when K atoms are attached (forming C–O–K groups), net charges decreased—i.e., electron populations increased. The increase in the electron density was more pronounced when the C–O–K groups were attached to the zigzag edges. The most significant increase occurred at C_{28}, the carbon atom connecting two C–O–K groups, with a net charge of −0.486. This is understandable because the bridge carbon atom received electrons from both K atoms.

From the results of the net charges, it was expected that the bridge carbon atom (that connects two C–O–K groups) would be the most favorable site for O chemisorption. For this reason, an O atom was added to C_{28} position in Fig. 5, and calculations were made to see how the C–C bond strengths were influenced. These C–C bonds must be broken for releasing CO for gasification. For comparison, O atoms were also added to similar positions on the armchair face (Structures 3 and 4 in Fig. 6).

The bond strengths, as expressed by diatomic energies, are shown in Tables 3 and 4. It is well known that CNDO *consistently* overestimates the bond energy. However, for the carbon and oxygen system, it is an empirical rule to divide the energy by a factor of ~5 for comparison with experimental bond energy (*40*). The values given in Tables 3 and 4 are sufficient nonetheless for comparison purposes. It is seen from Table 3 that the C–C bonds on the zigzag face were substantially weakened when O atoms were

TABLE 2

Net Charge (Electrons) of Carbon Atoms in Substrates with Armchair Edge (see Fig. 6)

Number	Structure 1	Structure 2	Number	Structure 1	Structure 2
15	0.1728	−0.0287	21	0.1751	−0.0038
16	0.0558	−0.0813	28	0.1728	−0.0287
17	0.2297	−0.0003	29	0.0558	−0.0813
18	0.1751	−0.0038	30	0.2297	−0.0003

TABLE 3

Carbon–Carbon Bond Strengths in Substrates with Zigzag Edge (Fig. 5), Expressed by Diatomic Energy (kcal/mol)

Bond	Structure 1	Structure 2	Structure 3	Structure 4
C_{28}–C_{29}	474.49	543.20	400.04	398.17
C_{28}–C_{30}	474.49	543.20	400.04	398.17
C_{12}–C_{29}	419.75	526.90	414.29	509.20
C_{24}–C_{30}	419.75	526.90	414.29	509.20

added to the bridge carbon atoms (C_{28}), bridging both C–O and C–O–K groups. As a consequence, the C–C bonds could be easily broken for gasification to take place. The question still remained as to why C–O–K catalyzed the reaction, because the C–C bonds were equally weakened in both Structures 3 and 4 (Fig. 5 and Table 3). The answer to this question lied in the high negative charge on the bridge carbon atom (C_{28}) for Structure 4, see Table 1. The bridge carbon between two C–O–K groups was more favorable for O chemisorption than that between two C–O groups. Consequently, more oxygen chemisorption on the bridge carbon atom would occur with the presence of potassium. The rate of carbon gasification should be directly proportional to the concentration of the C(O) species on the bridge carbon.

The catalytic mechanism described above can also explain the well known observation reported in the literature that the activation energies were not changed in the alkali and alkaline earth catalyzed carbon gasification reactions by H_2O and CO_2 (*41–46*). The CNDO results showed that with or without potassium, the C–C bonds on the surface (Structures 3 and 4 in Fig. 5) were equally weakened (Table 3). Therefore, one would not expect a decrease in the activation energy by potassium. However, the highly negative charge on the bridge carbon atom (Table 1, C_{28}) increased the density of the weakened C–C bonds by chemisorption of oxygen, resulting in an increased rate. The O atoms were supplied by dissociative chemisorption of H_2O or CO_2 on edge carbon sites (*1*) or potassium species (*32*).

The CNDO results for the armchair face were very different from that for the zigzag face. Results in Table 4 indicated that the C–C bonds on the armchair face were actually strengthened by the C–O–K groups (Structure 2), and that chemisorption of O atom on the bridge carbon (between two C–O–K groups) also strengthened the C–C bonds. Structure 3 (Table 4 and Fig. 6) was the favorable intermediate for gasification on the armchair. These results indicated that the C–O–K groups should inhibit the gasification reaction. The inhibition of the

TABLE 4

Carbon–Carbon Bond Strengths in Substrates with Armchair Edge (Fig. 6), Expressed by Diatomic Energy (kcal/mol)

Bond	Structure 1	Structure 2	Structure 3	Structure 4
C_{16}–C_{31}	457.81	577.16	396.02	510.44
C_{29}–C_{32}	457.81	577.16	396.02	510.44
C_{31}–C_{32}	431.12	550.78	408.91	458.35

C–H_2O reaction by K_2CO_3 was actually observed in our laboratory (*47*), where the monolayer etch pits on the basal plane containing K_2CO_3 grew at a slower rate at 600°C. The pits were hexagonal, possibly bounded by armchair faces because these faces were inhibited (thus limiting the growth rate) according to the CNDO results. The inhibition was not observed in the experiments reported in the current work because all faces were zigzag faces; potassium was deposited on the zigzag faces which were preformed by the uncatalyzed reaction (Fig. 1).

Activity of Particles (Clusters)

In our previous study (*32*), the kinetics and mechanism of graphite gasification by H_2O and CO_2 catalyzed by five alkali and alkaline earth metal catalysts were investigated by studying the monolayer channeling action on the basal plane of graphite. It was concluded that CO_2 and H_2O were first dissociatively chemisorbed by these catalysts, followed by diffusion of O atoms/ions to the edge carbon sites, where breakage of C–C bonds took place to free CO. The C–C bond breakage was the rate-limiting step.

The recent study of Meijer *et al.* (*19*) indicated that the particles or clusters were anchored through C–O–K groups to the carbon surface. Our CNDO results, described above, further indicated that the amount and the rate of supply of O atoms to the bridge carbon atoms (bridging two C–O–K groups) on the zigzag face would determine the catalyzed gasification rate. The surface of the alkali clusters and particles were apparently more capable of dissociating H_2O and CO_2, as compared to the C–O–K groups and the uncovered edge carbon surface atoms. This higher dissociation activity of particles was consequently the reason for the fact that particles were more active than the C–O–K groups.

ACKNOWLEDGMENT

This work was supported by NSF Grant CTS-9120452.

REFERENCES

1. Walker, P. L., Jr., Rusinko, F., Jr., and Austin, L. G., *in* "Advances in Catalysis" (D. D. Eley, P. W. Selwood, and P. B. Weisz, Eds.), Vol. 11, p. 133. Academic Press, New York, 1959.

2. Walker, P. L., Jr., Shelef, M., and Anderson, R. A., *in* "Chemistry and Physics of Carbon" (P. L. Walker, Jr., Ed.), **4,** 287 (1968).

3. Wen, W. Y., *Catal. Rev. Sci. Eng.* **22,** 1 (1980).

4. McKee, D. W., *in* "Chemistry and Physics of Carbon" (P. L. Walker, Jr. and P. A. Thrower, Eds.), Vol. 16. Dekker, New York, 1981.

5. Yang, R. T., *in* "Chemistry and Physics of Carbon" (P. A. Thrower, Ed.), Vol. 19. Dekker, New York, 1984.

6. Wood, B. J., and Sancier, E. M., *Catal. Rev. Sci. Eng.* **26,** 233 (1984).

7. Baker, R. T. K., *in* "Carbon and Coal Gasification Science and Technology" (J. L. Figuereido and J. A. Moulijn, Eds.), NATO ASI Series E, No. 105, p. 231. Martinus Nijhoff, Dordrecht, 1986.

8. McKee, D. W., *Fuel* **62,** 170 (1983).

9. Veraa, M. J., and Bell, A. T., *Fuel* **57,** 194 (1978).

10. McKee, D. W., and Chatterji, S., *Carbon* **20,** 59 (1982).

11. Saber, J. M., Falconer, J. L., and Brown, L. F., *Fuel* **65,** 1356 (1986).

12. Mims, C. A., and Pabst, J. K., *Prepr. ACS Div. Fuel Chem.* **25**(3), 258 (1980).

13. Mims, C. A., and Pabst, J. K., *in* "Proceedings of the International Conference on Coal Science," p. 730. Verlag Gluckauf GmbH, Essen, 1981.

14. Freriks, I. L. C., Van Wechem, H. M. H., and Stuiver, J. C. M., *Fuel* **60,** 463 (1981).

15. Mims, C. A., Rose, K. D., Memchior, M. T., and Pabst, J. K., *J. Am. Chem. Soc.* **104,** 6887 (1982).

16. Mims, C. A., and Pabst, J. K., *Fuel* **62,** 176 (1983).

17. Yuh, S. J., and Wolf, E. E., *Fuel* **62,** 252 (1983).

18. Delannay, F., Tysoe, W. T., Heinemann, H., and Somorjai, G. A., *Carbon* **22,** 401 (1984).

19. Meijer, R., Weeda, M., Kapteijn, F., and Moulijn, J. A., *Carbon* **29,** 929 (1991).

20. Saber, J. M., Falconer, J. L., and Brown, L. F., *J. Catal.* **90,** 65 (1984).

21. Cerfontain, M. B., Meijer, R., Kapteijn, F., and Moulijn, J. A., *Carbon* **26,** 41 (1988).

22. Hennig, G. R., *J. Inorg. Nucl. Chem.* **24,** 1129 (1962).

23. Keep, C. W., Terry, S., and Wells, M., *J. Catal.* **66,** 451 (1980).

24. Carrazza, J., Chludzinski, J. J., Heinemann, H., Somorjai, G. A., and R. T. K. Baker, *J. Catal.* **110,** 74 (1988).

25. Pereira, P., Csencsits, R., Somorjai, G. A., and Heinemann, H., *J. Catal.* **123,** 463 (1990).

26. Yang, R. T., and Wong, C., *J. Catal.* **85,** 154 (1984).
27. Goethel, P. J., and Yang, R. T., *J. Catal.* **101,** 342 (1986).
28. Goethel, P. J., and Yang, R. T., *J. Catal.* **108,** 356 (1987).
29. Goethel, P. J., and Yang, R. T., *J. Catal.* **111,** 220 (1988).
30. Goethel, P. J., and Yang, R. T., *J. Catal.* **119,** 201 (1989).
31. Pan, Z. J., and Yang, R. T., *J. Catal.* **130,** 161 (1991).
32. Chen, S. G., and Yang, R. T., *J. Catal.*, in press.
33. Chu, X., Schmidt, L. D., Chen, S. G., and Yang, R. T., submitted for publication.
34. Spiro, C. L., McKee, D. W., Kosky, P. G., and Lamby, E. K., *Fuel* **62,** 180 (1983).
35. Lang, R. J., *Fuel* **65,** 1324 (1986).
36. Wigmans, T., Goebel, J. C., and Moulijn, J. A., *Carbon* **21,** 295 (1983).
37. Pople, J. A., and Beveridge, P. L., "Approximate Molecular Orbital Theory." McGraw–Hill, New York, 1970.
38. Sadlej, J., "Semiempirical Methods of Quantum Chemistry." Ellis Horwoord Ltd. Chichester, Poland, 1985.
39. Hojer, G., and Meza, S., *Acta Chem. Scand.* **36,** 3723 (1972).
40. Hayns, M. R., *Theoret. Chim. Acta (Berl.)* **39,** 61 (1975).
41. Kelemen, S. R., and Freund, H., *J. Catal.* **102,** 80 (1980).
42. Freund, H., *Fuel* **65,** 63 (1986).
43. Pereira, P., Csencsits, T., Somorjai, G. A., and Heinemann, H., *J. Catal.* **123,** 463 (1990).
44. Kapteijn, F., Peer, O., and Moulijn, J. A., *Fuel* **65,** 1371 (1986).
45. Freund, H., *Fuel* **64,** 657 (1985).
46. Cerfontain, M. B., Meijer, R., Kapteijn, F., and Moulijn, J. A., *J. Catal.* **107,** 173 (1987).
47. Wong, C., and Yang, R. T., *Ind. Eng. Chem. Fundam.* **23,** 298 (1984).